Electronic Supplementary Information

An anionic Na(I)–organic framework platform: separation of organic dyes and post-modification for highly sensitive detection of picric acid

Di-Ming Chen, Jia-Yue Tian, Zhuo-Wei Wang, Chun-Sen Liu,* Min Chen and Miao Du*

Henan Provincial Key Laboratory of Surface & Interface Science, Zhengzhou University of Light Industry, Zhengzhou 450002, P. R. China

E-mail: dumiao@zzuli.edu.cn; chunsenliu@zzuli.edu.cn

Chem. Commun.

Experimental details

Materials and methods. All chemicals of reagent grade were purchased and used without further purification. Analyses for C, H, and N were taken on a Perkin-Elmer 240 CHN elemental analyzer. IR was recorded in the range of 400–4000 cm^{-1} on a Bruker TENOR 27 spectrophotometer. Powder X-ray diffraction (PXRD) was carried out on a Rigaku D/Max-2500 X-ray diffractometer with Cu Kα radiation. Thermogravimetric analysis (TGA) was performed on a Labsys NETZSCH TG 209 Setaram apparatus with a heating rate of 10 °C/min in nitrogen atmosphere. Fluorescent spectra were obtained on an Agilent fluorescence spectrophotometer.

Preparation of $\{(Me_2NH_2^+)_5[Na_{31}(TATB)_{12}](DMF)_{25}(H_2O)_{67}\}_n$ (1). A mixture of H_3TATB (0.06 g, 0.16 mmol), $NaAlO_2$ (0.032 g, 0.4 mmol), and $HN(CH_3)_2$ (40%, aq) was dissolved in DMF (4 mL) in a screw-capped vial, which was heated at 100 °C for 96 h under autogenous pressure. Light yellow polyhedral crystals were produced after filtration, washed with DMF. Yield: 45% based on H_3TATB ligand. Elemental analysis (%) found (calcd) for: $C_{372}H_{493}Na_{31}N_{66}O_{164}$: C, 48.43 (48.76); H, 5.39 (5.01); N, 10.02 (10.67). IR (KBr, cm^{-1}): 3416(br), 1667(m), 1601(m), 1564(vs), 1518(m), 1357(vs), 1100(w), 1016(m), 883(w), 822(m), 777(w), 701(w), 492(w).

Preparation of $\{(Rh6G)(Me_2NH_2^+)_4[Na_{31}(TATB)_{12}](DMF)_{29}(H_2O)_{69}\}_n$ (Rh6G@1). A fresh sample of **1** (20 mg) was soaked into a DMF solution (10 mL) of Rh6G (0.1 mol/L) for two days, during which the dye solution was exchanged every 12 hours. After that, the solution was filtrated and washed with DMF solvent until no Rh6G could be detected in the filtrate (as monitored by UV-vis spectra). Elemental analysis (%) found (calcd) for $C_{383}H_{517}N_{69}Na_{31}O_{170}$: C, 46.69 (48.32); H, 5.14 (5.47); N, 10.33 (10.15). The TGA plot for **Rh6G@1** resembles that of **1** with a 35.2% weight loss from room temperature to 460 °C (Fig. S7), which reveals the exclusion of 29 DMF, 69 water, and 4 $HNMe_2^+$ (calcd: 35.9%).

X-ray crystallography. Data were collected on an Agilent Technologies SuperNova Single Crystal Diffractometer equipped with graphite-monochromatic Cu Kα radiation (λ = 1.54184 Å). The structure was solved by SHELXS (direct methods) and refined by SHELXL (full matrix least-squares techniques) in the Olex2 package. All non-hydrogen atoms were refined with anisotropic displacement parameters. Hydrogen atoms attached to carbon were placed in geometrically idealized posi-

tions and refined with a riding model. For the highly disordered nature of lattice guests, they could not be finely made out in the refinement, and thus the SQUEEZE routine of PLATON was applied to remove the diffraction contributed from the highly disordered guests. The chemical formula was determined by the combination of the crystal data, TGA result, and elemental analysis.

Table S1 Crystal data and structure refinement for **1**.

Empirical formula	$C_{388}H_{578}Na_{31}N_{71}O_{194}$
Formula weight	10053.9
Temperature / K	293(2)
Crystal system	Cubic
Space group	*F*-43c
a / Å	48.1642(8)
b / Å	48.1642(8)
c / Å	48.1642(8)
α /°	90
β /°	90
γ /°	90
Volume / Å^3	111731(5)
Z	8
ρ_{calc} / g cm^3	0.710
μ / mm^{-1}	0.640
F(000)	24328.0
Crystal size / mm^3	0.4 × 0.2 × 0.2
Radiation	Cu Kα (λ = 1.54184)
Reflections collected	15687
Independent reflections	7387 [R_{int} = 0.0604, R_{sigma} = 0.0594]
Data/restraints/parameters	7387/25/322
Goodness-of-fit on F^2	0.868
Final *R* indexes [$I >= 2\sigma (I)$]	R_1 = 0.0954, wR_2 = 0.2603
Final *R* indexes (all data)	R_1 = 0.1252, wR_2 = 0.2877
Largest diff. peak and hole / e Å^{-3}	0.41 and –0.26

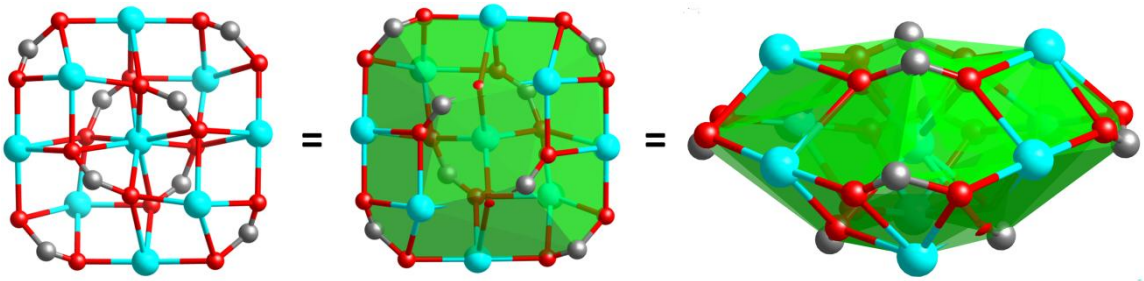

Fig. S1 The diamond-like nine nuclear Na(I)-based SBU in **1**.

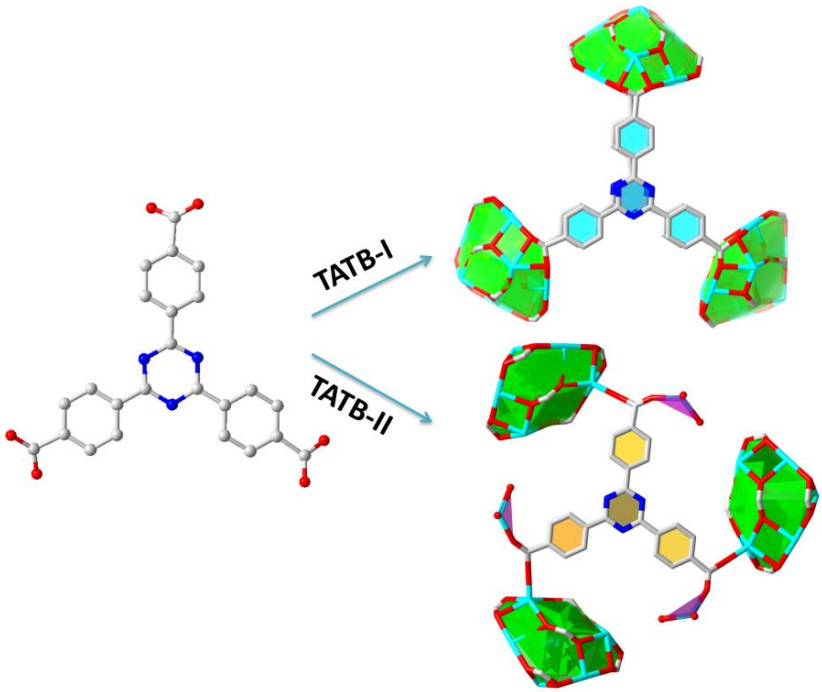

Fig. S2 Two different types of connection modes for the $TATB^{3-}$ ligands.

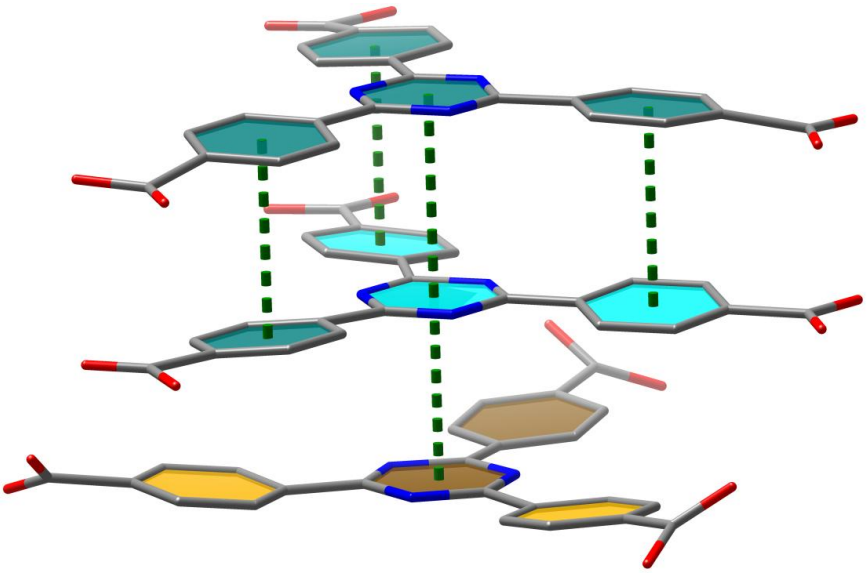

Fig. S3 The tightly packed $TATB^{3-}$ ligands in the crystal lattice of **1**.

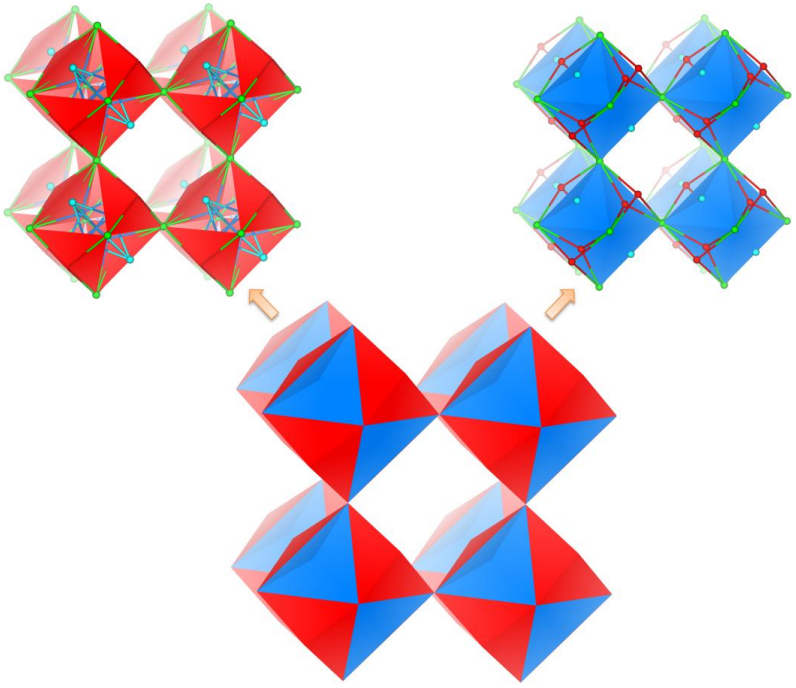

Fig. S4 View of the formation of the cages.

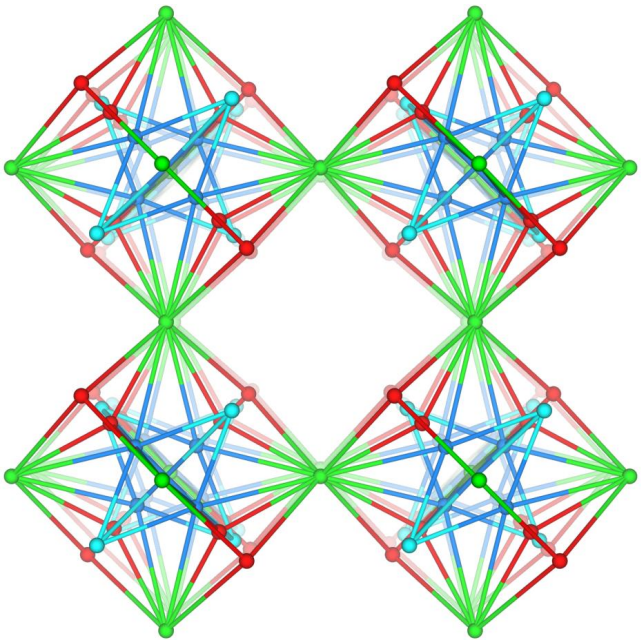

Fig. S5 The (3,6,12)-connected topological network for **1**.

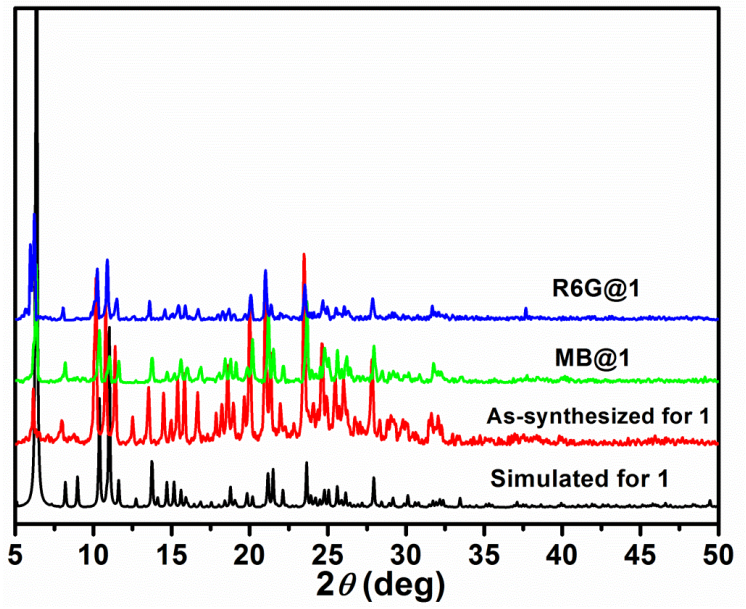

Fig. S6 PXRD patterns for **1**, **MB@1**, and **R6G@1**.

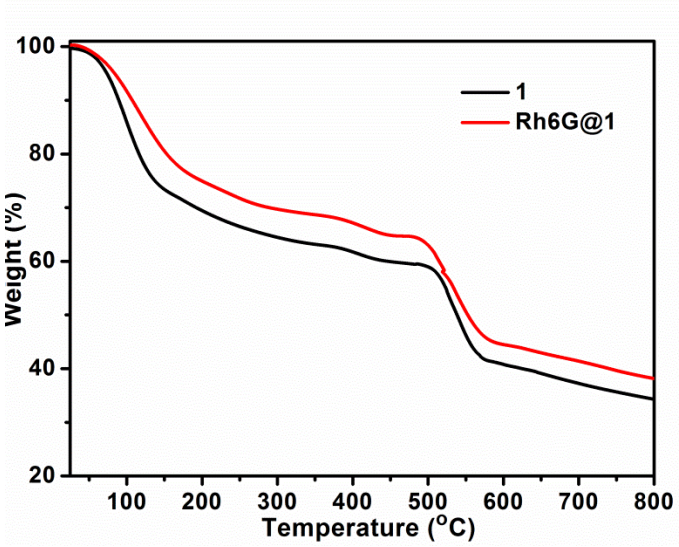

Fig. S7 The TGA curves for **1** and **Rh6G@1**.

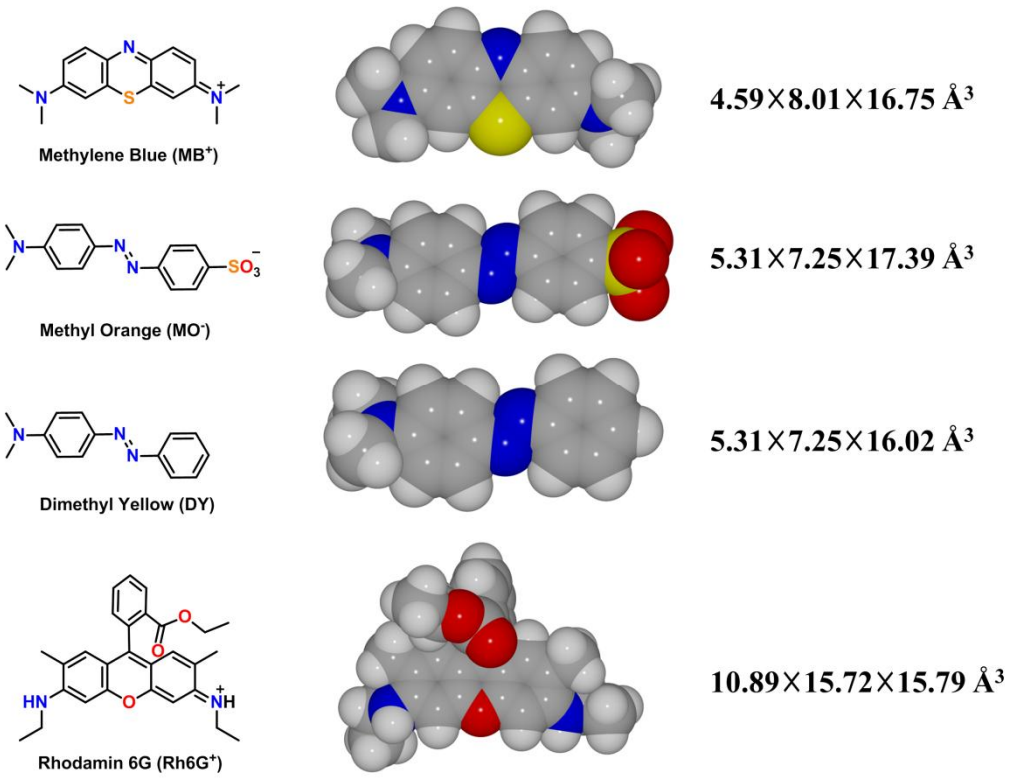

Fig. S8 The molecular structures and sizes of organic dyes (the molecular sizes of the dyes were derived from their geometry optimized structures in Forcite plus using the scale bar tool in the Material Studio software)

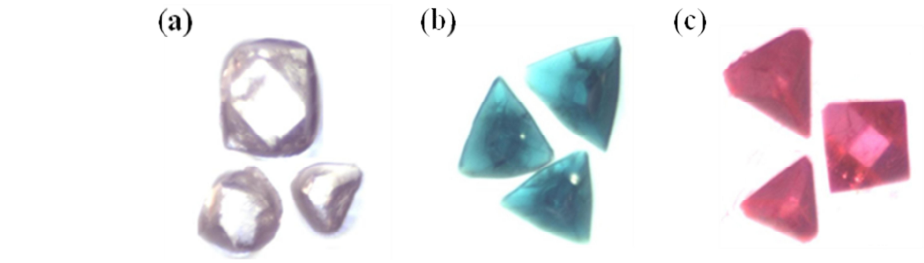

Fig. S9 The color changes of the crystals for **1** before (a) and after dye uptake (b: MB and c: Rh6G).

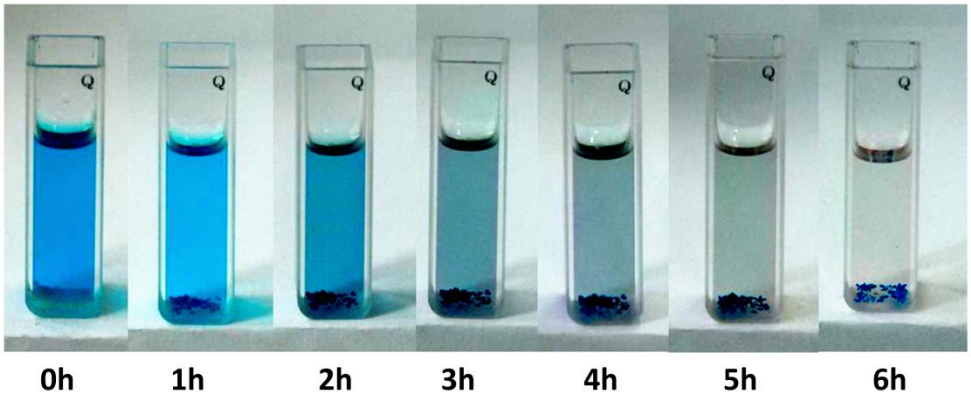

Fig. S10 The time dependent color change for the DMF solution of MB in the presence of **1**.

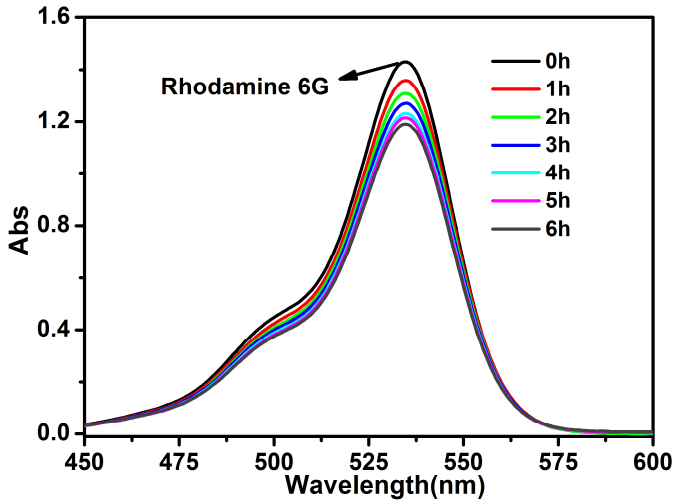

Fig. S11 Time-dependent UV-vis absorption spectra of Rh6G.

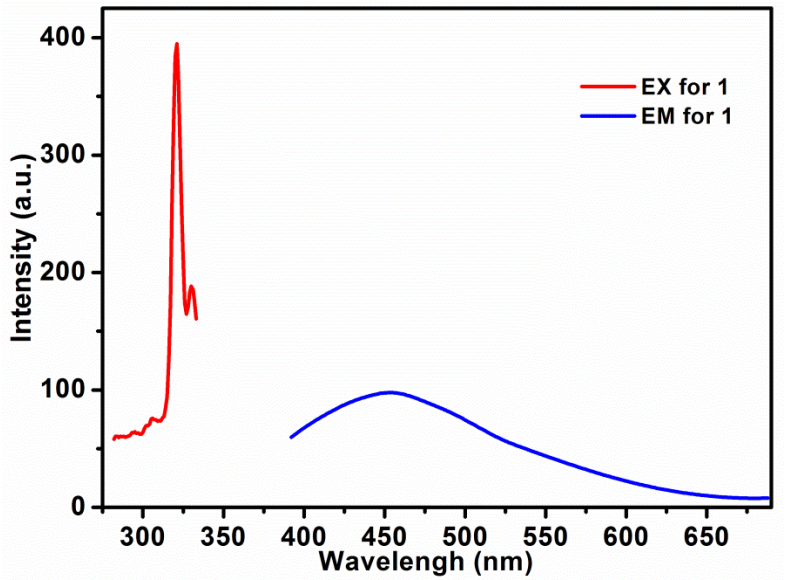

Fig. S12 Solid state excitation (red at 450 nm) and emission (blue at 320 nm) spectra of **1**.

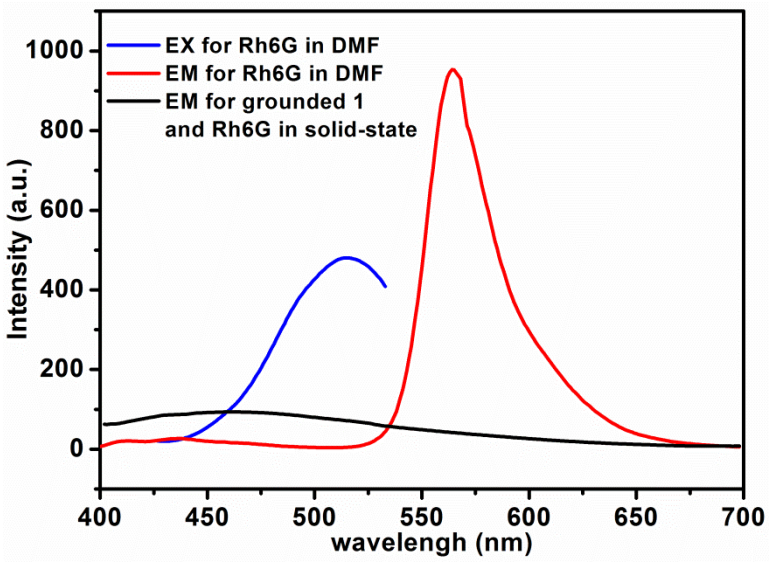

Fig. S13 Excitation (red at 450 nm) and emission (blue at 320 nm) spectra of Rh6G in DMF as well as the solid state emission (black at 320 nm) spectrum for the mixture of **1** and Rh6G.

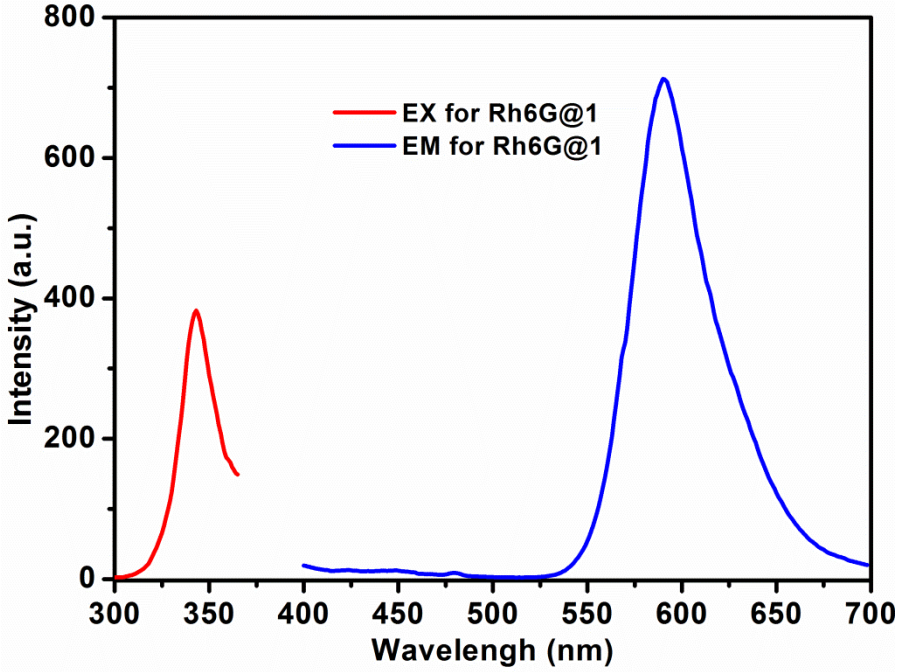

Fig. S14 Solid state excitation (red at 590 nm) and emission (blue at 338 nm) spectra of **Rh6G@1**.

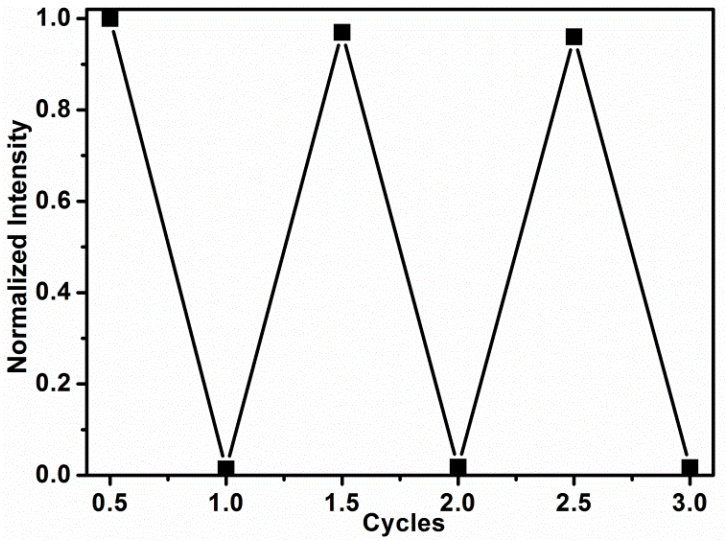

Fig. S15 The quenching and recovery test of **Rh6G@1**. The dots above and below are the initial luminescent intensity and the intensity upon adding 100 ppm DMF solution of PA.

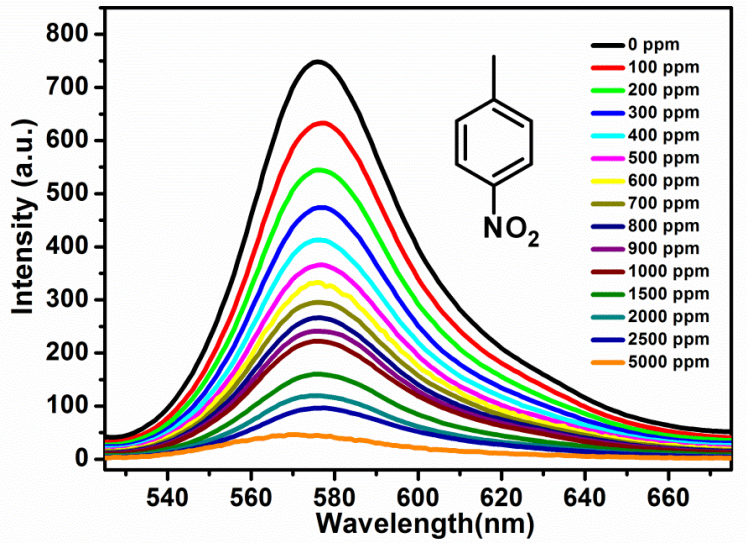

Fig. S16 Emission spectra of **Rh6G@1** upon the addition of *p*-nitrotoluene.

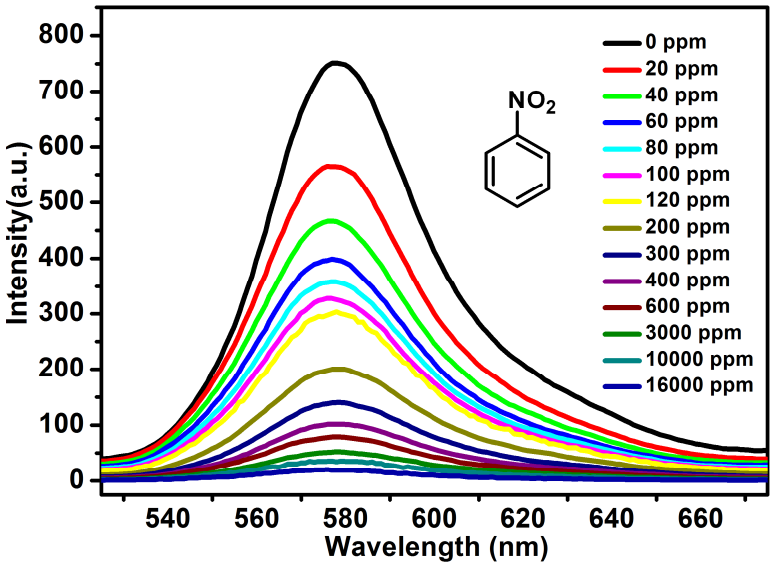

Fig. S17 Emission spectra of **Rh6G@1** upon the addition of nitrobenzene.

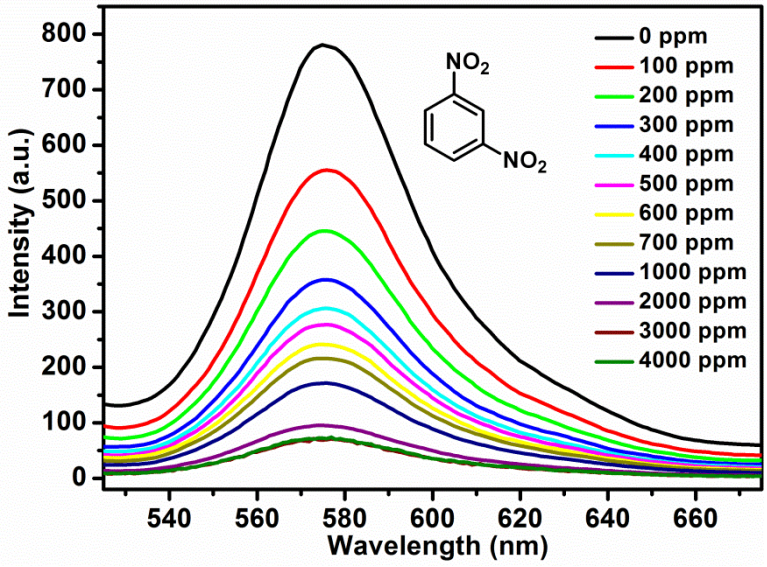

Fig. S18 Emission spectra of **Rh6G@1** upon the addition of *m*-dinitrobenzene.

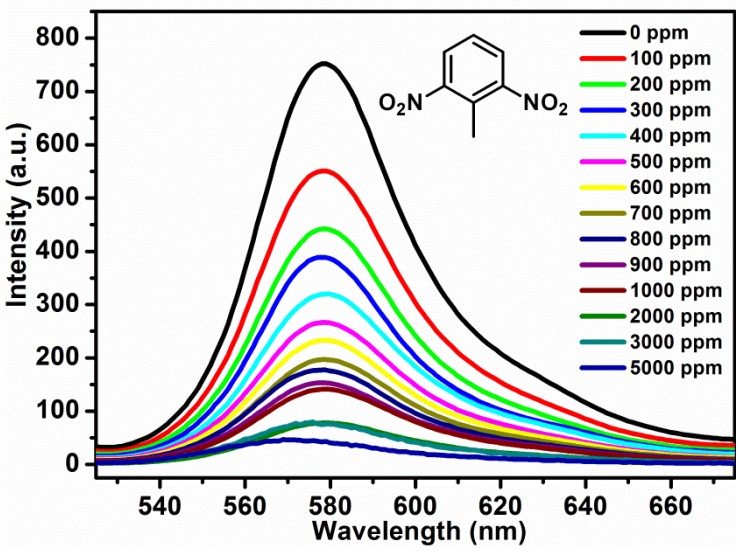

Fig. S19 Emission spectra of **Rh6G@1** upon the addition of 2,6-dinitrotoluene.

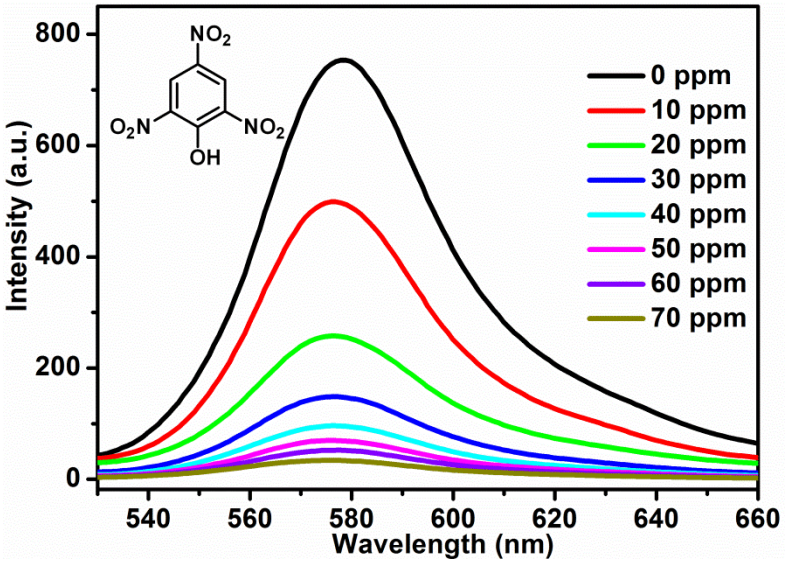

Fig. S20 Emission spectra of **Rh6G@1** upon the addition of PA.

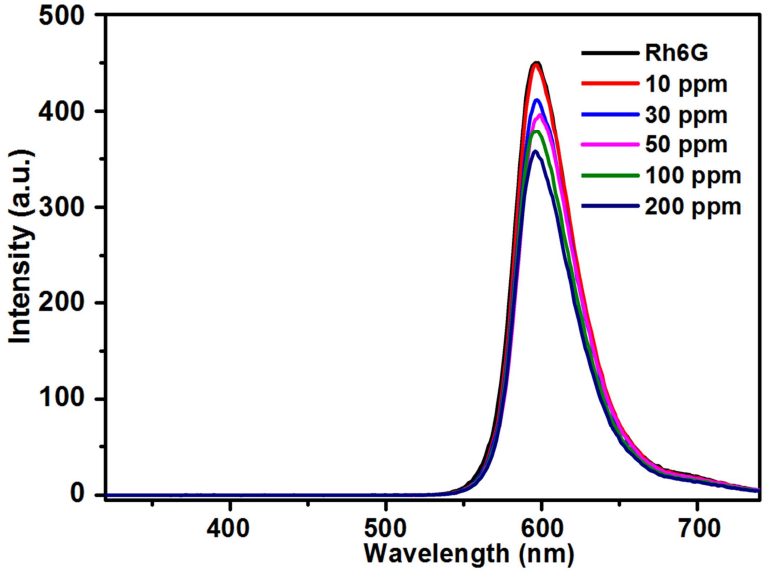

Fig. S21 Emission spectra of **Rh6G** upon the addition of PA.

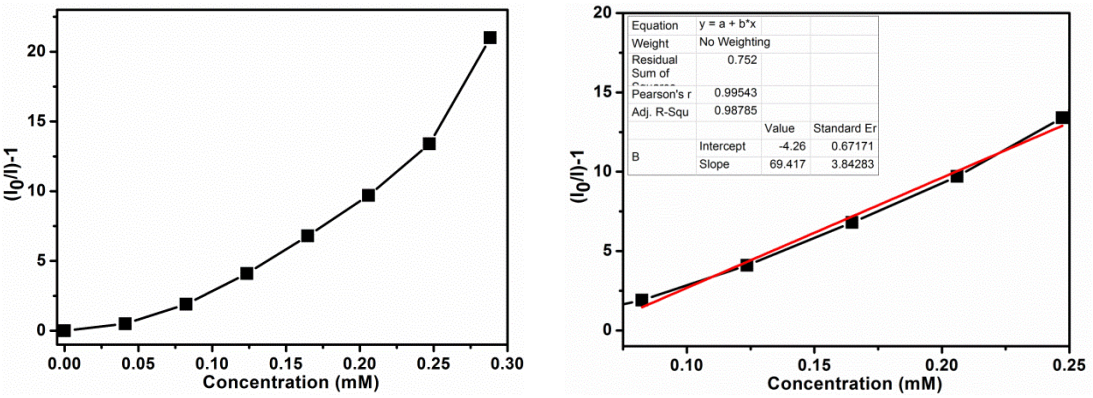

Fig. S22 Stern-Volmer plot for the fluorescence quenching of **Rh6G@1** upon addition of PA (left) and Stern-Volmer plot at low PA concentrations (right).

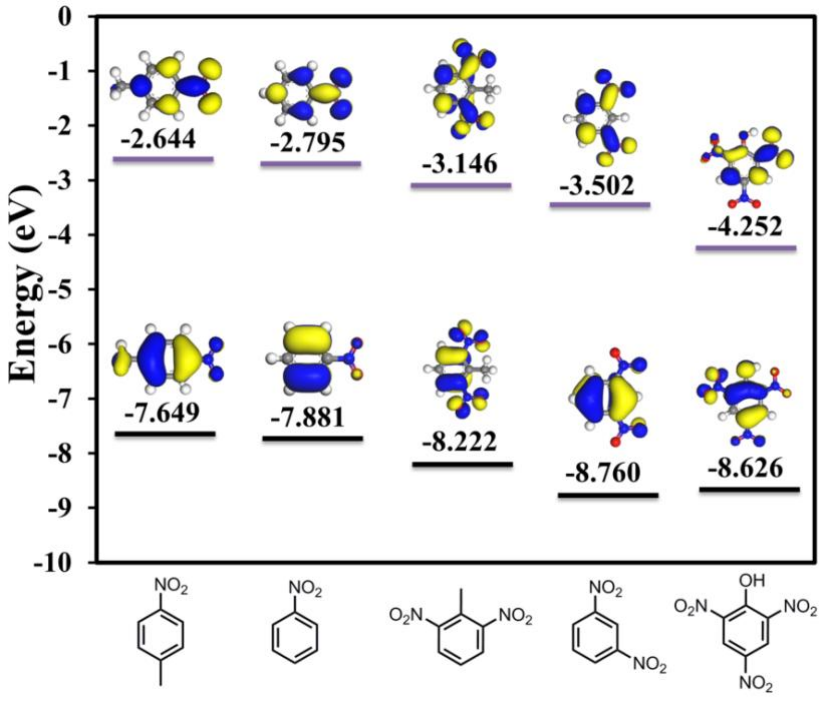

Fig. S23 The DFT calculated HOMO and LUMO energies of the nitro analytes at the B3LYP/6-31G* level.

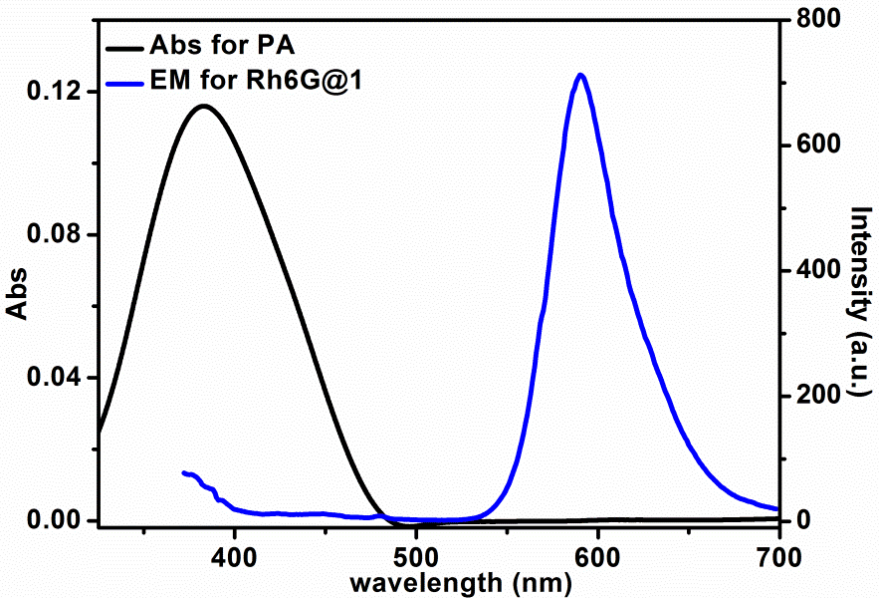

Fig. S24 Comparison of the emission spectrum of **Rh6G@1** and absorption spectrum of PA.